POTENTIAL BRINE-LITHIUM-BEARING REGIONS DETECTION AND MAPPING USING A MODIFIED DEEP LEARNING SELF-SUPERVISED UNMIXING-BASED APPROACH OF MULTI- AND HYPERSPECTRAL DATA

Fatima Zohra Benhalouche, *Oussama Benabbou*, *Moussa Sofiane Karoui*, *Ahmed Bennia* and *Lahsen Wahib Kebir*

Agence Spatiale Algérienne, Centre des Techniques Spatiales, Arzew, Algeria

ABSTRACT

Chotts are complex sedimentary environments because the minerals of interest they contain are often diffuse and mixed with other evaporitic deposits. This paper presents a new study on the detection and mapping of potential brine-lithium-bearing regions in an Algerian Chott. The employed methodology is based on a modified self-supervised deep learning framework applied on remote sensing multispectral Landsat-8 and hyperspectral PRISMA and EnMAP data. The considered unmixing-based framework uses the endmember-guided unmixing network. Based on a two-stream architecture, this model, which considers the spectral variability phenomenon, makes it possible to extract pure endmember spectra and estimate their abundance maps. The obtained results demonstrate that the used approach effectively maps areas of evaporite concentration, particularly gypsum salt and carnallite, which are considered as indirect indicators of Lithium potential.

Index Terms— Mineral mapping, multispectral Landsat-8 and PRISMA/EnMAP hyperspectral remote sensing data, spectral unmixing, spectral variability, modified self-supervised deep learning, two-stream endmember-guided network.

1. INTRODUCTION

Algerian Chotts, such as “Melrhir” and “Merouane” ones, constitute environments of major interest for mining, due to their function as endorheic basins that promote the concentration of strategic mineral resources [1].

In arid/semi-arid climates, the processes of bedrock weathering, hydrological transport, and intense evaporation lead to the accumulation of brines and evaporite sediments rich in economically valuable minerals, such as Salt and Gypsum, as well as critical elements like Lithium, Boron, and Potassium [2].

In such environments, Lithium is of secondary origin and exists in a diffuse form. It is absorbed or incorporated into evaporitic clays and some secondary minerals within brines and evaporitic sediments [2], [3]. This diffuse distribution, combined with the relative homogeneity of surfaces, complicates its direct detection, making remote sensing a valuable tool for its indirect detection and mapping.

Indeed, the potential of space-based remote sensing data for mineral detection and mapping has been extensively explored over the past twenty years [4]-[6]. These studies have concentrated on mapping alteration zones or directly identifying minerals of interest, especially in expansive or hard-to-reach areas, thereby optimizing the time spent on mineral exploration [7]-[8].

Recently, hyperspectral remote sensing sensors have been receiving increasing attention due to their high spectral resolution, which allows for more accurate identification and classification of surface mineralogy. As a result, several methods applied to these data, have been proposed for the detection and mapping of various minerals, particularly those that are sparsely abundant on the surface [8]-[10].

However, direct detection of minerals using hyperspectral data remains a challenge due to their limited spatial resolution. Indeed, the low spatial resolution of hyperspectral sensors results in mixed spectra within pixels, making accurate identification of materials difficult and requiring additional processing to separate these mixed spectra.

Linear Spectral Unmixing (LSU) is a technique commonly used for hyperspectral data analysis [11]. LSU aims to estimate, for each pixel in an image, pure endmember spectra and their abundance fractions, which represent the relative proportions of each material in each pixel of the processed image.

Most standard Linear Mixing Models (LMM) [11] used in LSU techniques are based on the assumption that each pure endmember is represented by a unique spectrum that is invariant across the entire image. However, this assumption is often too simplistic for real-world scenes.

In practice, spectra are subject to significant spectral variability, from one pixel to another, due to several factors: variations in illumination, atmospheric effects, land topography, instrumental noise, and nonlinear mixing phenomena [12], [13].

Faced with these complexities, new methods based on Deep Learning (DL) have emerged [14]-[17]. These DL-based approaches take advantage of machine learning through deep neural network architectures. Supervised ones require large labeled training datasets and may not generalize well to datasets not included in the training process, while unsupervised methods learn directly from the input data.

Besides, a study reported in [18] proposed a new approach based on a LMM that explicitly takes into account the phenomenon of spectral variability [19]. Based on nonnegative matrix factorization [20], this approach relies on an informed and penalized hyperspectral unmixing algorithm, aimed at improving the estimation of abundance fraction maps of materials of interest by exploiting their known spectra. In [18], this approach is used for detecting and mapping potential pegmatite-lithium-bearing deposit areas using remote sensing hyperspectral PRISMA data.

In this investigation, the self-supervised DL-unmixing-based approach proposed in [21], [22], which is based on a two-stream architecture, called Endmember-Guided Unmixing Network (EGU-Net), is modified and employed for detecting and mapping brine-lithium-bearing areas, based on indirect

indicators derived from Landsat 8 multispectral data and PRISMA and EnMAP hyperspectral data. More precisely, the employed approach is adapted to directly exploit the known spectra of indirect indicators of Lithium presence. Moreover, this approach models spectral variability by learning multiple representations of endmembers and integrating them into the overall unmixing process. In addition, it includes physical constraints on abundance fractions.

The novelty of this work lies in the integration of: *i*) a modified self-supervised deep unmixing, *ii*) multi-sensor data (Landsat-8, PRISMA, EnMAP), and *iii*) domain-driven selection of Lithium indicator minerals. This combination has not been explored for brine Lithium exploration in Chotts. Furthermore, this work is not a simple experiment, but a study of methodological adaptation and application with geoscientific implications. The work conducted at this stage builds on the reference study presented in [2], which has already involved field surveys and geochemical analyses in the study area.

The framework proposed in this paper is not tied to a specific region but is based on spectral decomposition and prior spectral knowledge of indicator minerals. Therefore, this work can be applied to other evaporitic environments where similar hydrochemical processes occur.

The remainder of this paper is organized as follows. Section 2 provides a description of the considered self-supervised EGU-Net unmixing approach. In Section 3, the used data and study area are described. The obtained results are presented in Section 4. Finally, a conclusion is given in Section 5.

2. CONSIDERED MODIFIED DEEP LEARNING SELF-SUPERVISED EGU-NET UNMIXING APPROACH

As introduced, the approach used in this work is a modified version of the one presented in [21]. It aims to model and analyze spectral variability in the context of spectral unmixing [17]. It is also able to take into account nonlinear effects while remaining physically interpretable. Indeed, EGU-Net, proposed in [21], improves hyperspectral unmixing by overcoming the limitations of the standard linear model. It combines two key approaches: first, the incorporation of quadratic terms to model complex physical interactions (reflections, scattering), and then, the use of a Siamese-based deep learning architecture [21]. Unlike traditional models, EGU-Net processes spectral signatures as dynamic rather than fixed variables, enabling precise and adaptive management of spectral variability for each pixel.

The hyperspectral observation $Y \in \mathbb{R}_+^{L\times P}$ is modeled as a product of the endmember signatures and the abundance maps, subjected to a latent transformation by the encoder

$$Y = E \cdot \sigma\big(f_{\Phi}(Y,E)\big), \tag{1}$$

where $f_{\Phi}(Y,E)$ represents the encoder function with weights Φ. This encoder function is considered as fractional abundances. $\sigma(\cdot)$ is the softmax activation function, which ensures the sum-to-one and nonnegativity constraints. $E \in \mathbb{R}_+^{L\times N}$ is the endmember matrix. N is the number of endmembers (pure materials), P is the number of pixels, and L represents the number of spectral bands of the considered image.

The unmixing process is thus formulated as a constrained optimization problem, incorporating regularizations ensuring the stability and interpretability of the solutions [21].

The optimized criterion is based on the reconstruction error between the observed image and the reconstructed image produced by the proposed model. The optimization is based on an iterative method of alternating gradient descent, where abundances are updated by fixing the endmembers, then the endmembers are updated by fixing the abundances.

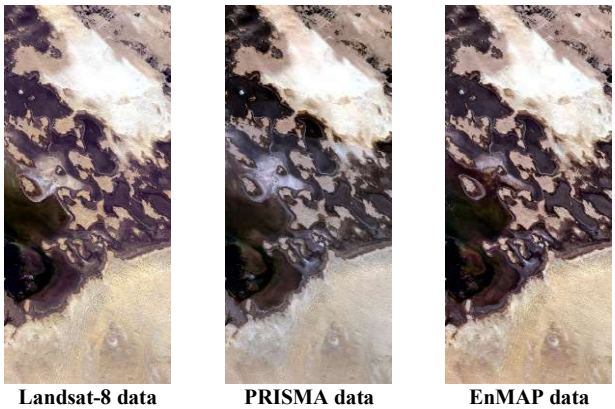
In this investigation, the original approach [21] is adapted, rather than applied directly, to better address specific research objectives, particularly regarding the spectral extraction process. More precisely, the processed data are segmented into partially overlapping blocks, whose size is set by default to 5×5 pixels, and for each block, the number of pure materials is automatically estimated by means of the HySime algorithm [11], then the endmember spectra are extracted by applying the vertex component analysis method [11]. Then, the spectra are categorized, via a clustering algorithm, such as *k*-means [23], into two distinct groups: a first group of known spectra, containing in the matrix E_1 and comprising materials identified as indirect indicators of Lithium presence, whose characteristics are strictly preserved as initially introduced in the considered unmixing technique, and a second group of assumed unknown spectra containing in the matrix E_2, which are iteratively updated by the network. Therefore, the matrix E becomes as described in [18]

$$E = E_1 + E_2. \tag{2}$$

The abundance maps are then estimated following the procedure described in [21].

3. USED DATA AND STUDY AREA

In this work, multispectral VNIR-SWIR Landsat-8, hyperspectral PRISMA [24] and EnMAP [25] data (Figure 1) are used. These data were acquired between December 2024 and January 2025, with a spatial resolution of 30 meters. These data, which cover two Algerian Chotts, are geometrically and atmospherically corrected.



Landsat-8 data acquired on December 14, 2024 | **PRISMA data acquired on December 07, 2024** | **EnMAP data acquired on January 08, 2025**

Figure 1. RGB color composites of the used Landsat-8, PRISMA and EnMAP data.

Besides, 6 spectral bands, in the 0.45-2.29 µm spectral range, of the Landsat-8 data, were considered. Also, from the 234 spectral bands, in the 0.4-2.5 µm spectral domain, of the considered PRISMA hyperspectral data, only 103 bands, which show the lowest anomalies in terms of noise and calibration, are selected. Furthermore, all available EnMAP spectral bands, in the 0.5-2.5 µm spectral domain, were considered.

In this investigation, the considered study area is located in Central-Eastern Algeria (Figure 2) and concerns the two ephemeral salt lakes "Melrhir" and "Merouane" Chotts: two endorheic systems in the Northern Sahara sedimentary basin in the South of the Saharan Atlas. These two Chotts are characterized by intermittent hydrology, high evaporation, and high salinity, with evaporite deposits dominated by Halite, Gypsum, and Carbonates. Their water supply is mainly provided by the Northwestern Sahara Aquifer System (NWSAS), supplemented by occasional rainfall [3].

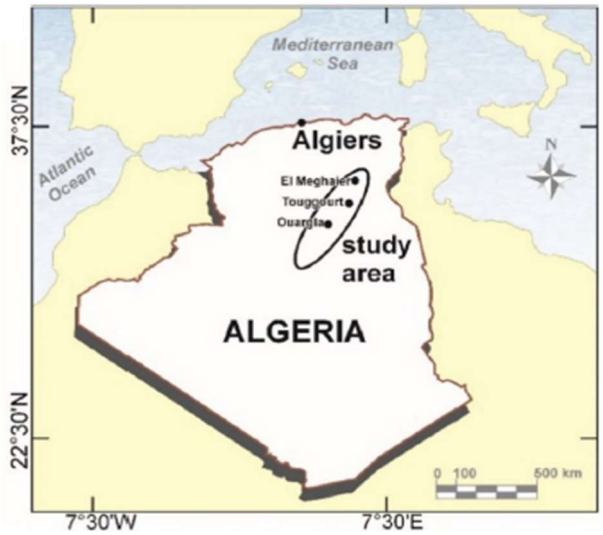


Figure 2. The location of the considered study area: "Melrhir" and "Merouane" Chotts [2].

It should be noted that the specific hydrochemical conditions of these environments favor the formation of saline minerals and the enrichment of lake sediments with Lithium.

Indeed, salinity gradients strongly control the distribution of halophyte vegetation.

Despite their ecological and geochemical interest, these two Chotts remain poorly studied, and therefore the present work aims to contribute to their analysis through the processing of remote sensing data.

Moreover, it should be noted that the considered remote sensing data were all selected between December and January to take into account seasonal variations in the water level of these two Chotts, a period during which the lakes are fed by precipitation and groundwater, while ensuring low (less than 10%) cloud cover.

As the DL-unmixing-based method used in this work includes, in addition to spectra automatically estimated, known spectra of relevant materials to be detected and mapped, these were selected from spectral libraries [26] in order to best match the characteristics of the processed data and prior knowledge about the materials present in the study area.

Besides, these spectra were spectrally resampled to coincide with spectral bands of each processed multi- and hyperspectral image.

Furthermore, in this investigation, six materials of interest, whose spectra are assumed to be known (Figure 3), are considered. These materials are: Carnallite, Water bodies, Vegetation, Salt, Gypsum and Sand.

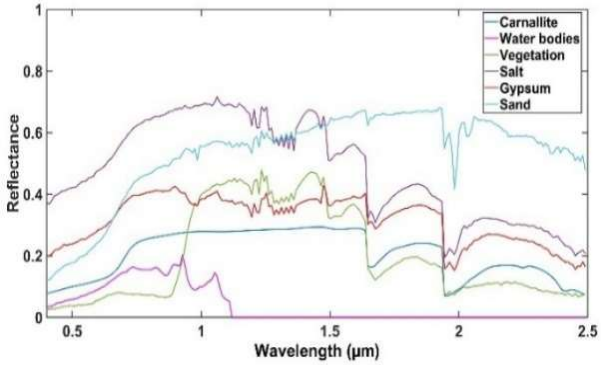


Figure 3. The considered known material spectra.

4. OBTAINED RESULTS

The considered modified self-supervised DL-unmixing-based approach is applied to the above-described data to estimate, in particular, the abundance fraction maps of the above defined materials of interest whose spectra are considered as known.

The following figure (Figure 4) illustrates the obtained abundance fraction maps.

These abundance maps highlight the decisive role of evaporative dynamics in the Saharan context, where evaporation controls the mineralogical organization of the two considered Chotts. Early precipitating-Salts, such as Halite and Gypsum, crystallize rapidly, while Lithium gradually concentrates in the residual brine during the most advanced stages of evaporation.

Although Lithium is not directly detectable by remote sensing data, mapping indirect indicators, particularly Carnallite, makes it possible to identify areas favorable to its accumulation.

The processed data, in particular the hyperspectral ones, reveal a localized and fragmented distribution of Carnallite, mainly in the center of the two Chotts, particularly in the "Hamraya" sector, confirming the existence of a geochemical anomaly. This weak surface expression may be linked to masking by more abundant salts.

Besides, Figure 4 also shows that the abundance maps obtained from EnMAP data offer relatively better discrimination of extreme evaporitic stages. Indeed, the Salt map highlights a central area of advanced Salt crystallization, contrasting with less pronounced peripheral areas influenced by humidity and sedimentary mixtures.

Gypsum is more widely distributed, corresponding to intermediate evaporitic phases and structuring the spatial organization of the two Chotts.

The sandy formations located on the periphery reflect detrital inputs, while Water bodies and Wetlands are concentrated in the lower parts of the basin, indicating preferential accumulations of brine.

Finally, Vegetation, which is very limited in terms of space, is better discriminated by the used PRISMA and EnMAP hyperspectral data, making it possible to distinguish vegetated areas from wet soils.

Globally, Figure 4 shows that the combination of the used modified DL-unmixing-based approach and hyperspectral data improves spectral discrimination, enabling the effective identification of areas of hydrological convergence, which are essential to the functioning of the evaporite system and the location of areas potentially enriched with lithium-bearing brines.

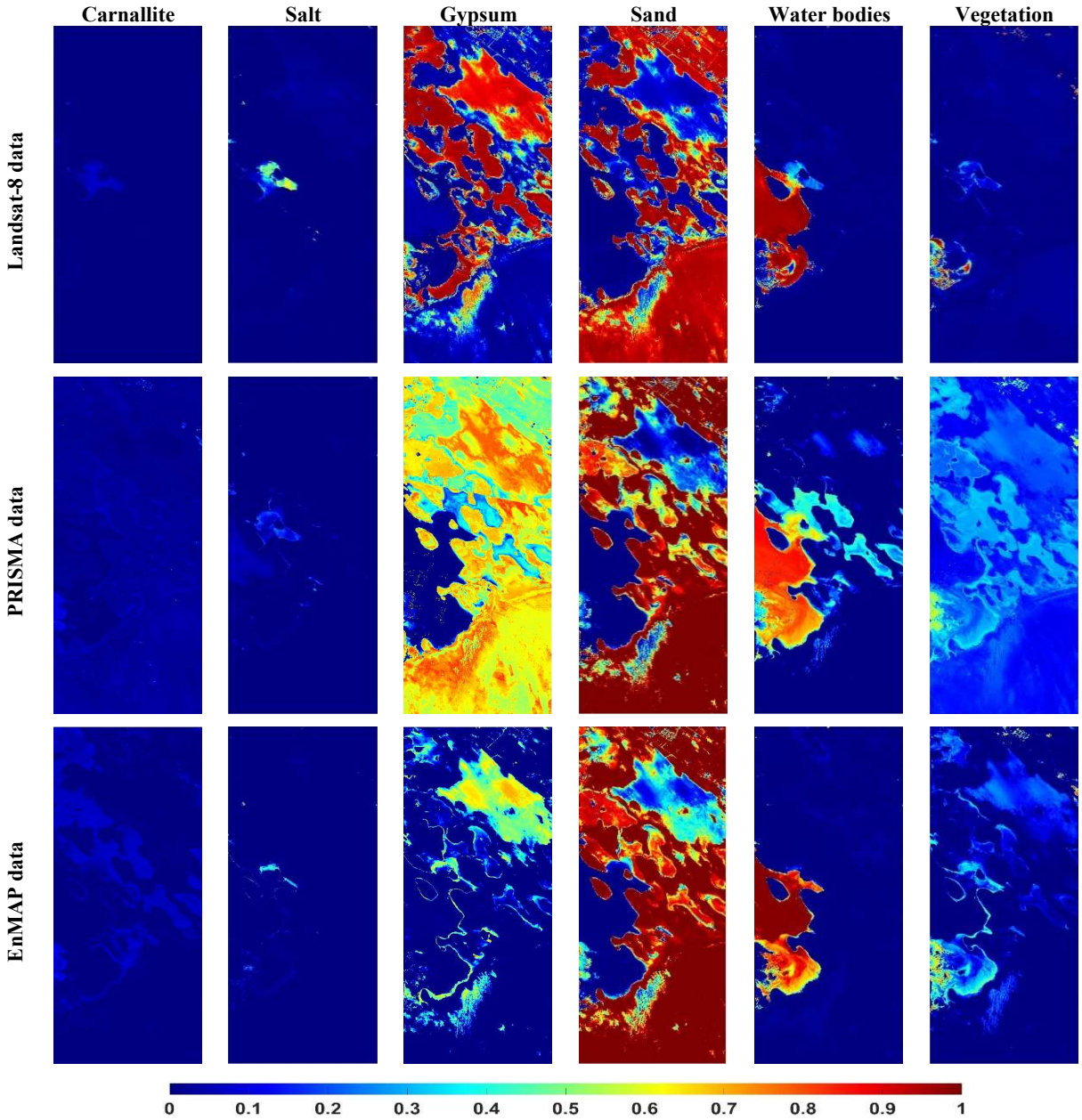


Figure 4. Obtained abundance fraction maps, from the considered data, of minerals of interest whose spectra are known.

5. CONCLUSION

This study highlights the effectiveness of the considered modified deep learning self-supervised unmixing network, called EGU-Net, in addressing the challenge of detecting and mapping brine-lithium-bearing areas in complex environments.

By integrating Landsat-8 multispectral, PRISMA and EnMAP hyperspectral data into a deep learning framework, the used modified approach makes it possible to manage the spectral variability of surface deposits in Chotts and improve the mapping of indirect indicators of Lithium presence, such as Carnallite, Salt and Gypsum, which reveal evaporitic dynamics.

The model's ability to estimate mineral abundances from satellite data thus provides a valuable pre-exploration tool, reducing geological uncertainties and effectively directing future Lithium exploration campaigns towards the most promising areas of the “Melrhir” and “Merouane” Chotts.

6. REFERENCES

[1] M. Hacini, E. H. Oelkers, and N. Kherici, "Retrieval and interpretation of precipitation rates generated from the composition of the Merouane Chott ephemeral lake," J. Geochem. Explor., vol. 88, no. 1–3, pp. 284–287, Jan. 2006, doi: 10.1016/j.gexplo.2005.08.057.

[2] M. Zatout et al., "Saharan lithium: Brine chemistry of chotts from eastern Algeria," Appl. Geochem., vol. 115, p. 104566, Apr. 2020, doi: 10.1016/j.apgeochem.2020.104566.

[3] F. Remita et al., "Major Ionic Evolution of Na–Mg–Cl Brines in Solar Saltworks and Their Processing Optimization: A Case Study from Chott Melrhir Salt Lake, Algeria," Geol. J., vol. 60, no. 8, pp. 1825–1839, Aug. 2025, doi: 10.1002/gj.5232.

[4] S. Chabrillat et al., "Use of hyperspectral images in the identification and mapping of expansive clay soils and the role of spatial resolution," Remote Sens. Environ., vol. 82, no. 2–3, pp. 431–445, Oct. 2002, doi: 10.1016/S0034-4257(02)00060-3.

[5] A. B. Pour et al., "Lithological and alteration mineral mapping in poorly exposed lithologies using Landsat-8 and ASTER satellite data: North-eastern Graham Land, Antarctic Peninsula," Ore Geol. Rev., vol. 108, pp. 112–133, May 2019, doi: 10.1016/j.oregeorev.2017.07.018.

[6] H. Shirmard et al., "A review of machine learning in processing remote sensing data for mineral exploration," Remote Sens. Environ., vol. 268, p. 112750, Jan. 2022, doi: 10.1016/j.rse.2021.112750.

[7] S. Gabr, A. Ghulam, and T. Kusky, "Detecting areas of high-potential gold mineralization using ASTER data," Ore Geol. Rev., vol. 38, no. 1–2, Art. no. 1–2, Oct. 2010, doi: 10.1016/j.oregeorev.2010.05.007.

[8] R. D. M. Scafutto, C. R. De Souza Filho, and W. J. De Oliveira, "Hyperspectral remote sensing detection of petroleum hydrocarbons in mixtures with mineral substrates: Implications for onshore exploration and monitoring," ISPRS J. Photogramm. Remote Sens., vol. 128, pp. 146–157, Jun. 2017, doi: 10.1016/j.isprsjprs.2017.03.009.

[9] R. Booysen et al., "Accurate hyperspectral imaging of mineralised outcrops: An example from lithium-bearing pegmatites at Uis, Namibia," Remote Sens. Environ., vol. 269, p. 112790, Feb. 2022, doi: 10.1016/j.rse.2021.112790.

[10] J. Cardoso-Fernandes et al., "Detecting Lithium (Li) Mineralizations from Space: Current Research and Future Perspectives," Appl. Sci., vol. 10, no. 5, p. 1785, Mar. 2020, doi: 10.3390/app10051785.

[11] J. M. Bioucas-Dias et al., "Hyperspectral Unmixing Overview: Geometrical, Statistical, and Sparse Regression-Based Approaches," IEEE J. Sel. Top. Appl. Earth Obs. Remote Sens., vol. 5, no. 2, Art. no. 2, Apr. 2012, doi: 10.1109/JSTARS.2012.2194696.

[12] A. Zare and K. C. Ho, "Endmember Variability in Hyperspectral Analysis: Addressing Spectral Variability During Spectral Unmixing," IEEE Signal Process. Mag., vol. 31, no. 1, Art. no. 1, Jan. 2014, doi: 10.1109/MSP.2013.2279177.

[13] R. A. Borsoi et al., "Spectral Variability in Hyperspectral Data Unmixing: A Comprehensive Review," IEEE Geosci. Remote Sens. Mag., vol. 9, no. 4, Art. no. 4, Dec. 2021, doi: 10.1109/MGRS.2021.3071158.

[14] B. Palsson et al., "Hyperspectral Unmixing Using a Neural Network Autoencoder," IEEE Access, vol. 6, pp. 25646–25656, 2018, doi: 10.1109/ACCESS.2018.2818280.

[15] S. S. Vijayashekhar, V. S. Deshpande, and J. S. Bhatt, "A Practical Approach for Hyperspectral Unmixing Using Deep Learning," IEEE Geosci. Remote Sens. Lett., vol. 19, pp. 1–5, 2022, doi: 10.1109/LGRS.2021.3127075.

[16] Y. Su et al., "Deep Autoencoders with Multitask Learning for Bilinear Hyperspectral Unmixing," IEEE Trans. Geosci. Remote Sens., vol. 59, no. 10, pp. 8615–8629, Oct. 2021, doi: 10.1109/TGRS.2020.3041157.

[17] Y. Cheng et al., "Hyperspectral Unmixing Network Accounting for Spectral Variability Based on a Modified Scaled and a Perturbed Linear Mixing Model," Remote Sens., vol. 15, no. 15, p. 3890, Aug. 2023, doi: 10.3390/rs15153890.

[18] F. Z. Benhalouche et al., "Detecting and Mapping Potential Pegmatite-Lithium-Rich Areas by an Unmixing-Based Approach Using Hyperspectral Prisma Data," in IGARSS 2025 - 2025 IEEE International Geoscience and Remote Sensing Symposium, Brisbane, Australia, Aug. 2025, pp. 2268–2272. doi: 10.1109/IGARSS55030.2025.11243853.

[19] M. S. Karoui, F. Z. Benhalouche, and Y. Deville, "Hyperspectral Unmixing with a Modified Augmented Linear Mixing Model Addressing Spectral Variability," in M2GARSS 2022 - 2022 IEEE Mediterranean and Middle East Geoscience and Remote Sensing Symposium, Virtual Symposium, Mar. 2022.

[20] A. Cichocki et al., Nonnegative matrix and tensor factorizations: Applications to exploratory multi-way data analysis and blind source separation. John Wiley and Sons, 2009.

[21] D. Hong et al., "Endmember-Guided Unmixing Network (EGU-Net): A General Deep Learning Framework for Self-Supervised Hyperspectral Unmixing," IEEE Transactions on Neural Networks and Learning Systems, vol. 33, no. 11, pp. 6518–6531, 2021. doi: 10.1109/TNNLS.2021.

[22] R. B. Lyngdoh et al., "Hyperspectral Unmixing with Spectral Variability Using Endmember Guided Probabilistic Generative Deep Learning," in IGARSS 2022 - 2022 IEEE International Geoscience and Remote Sensing Symposium, Kuala Lumpur, Malaysia, Jul. 2022, pp. 1768–1771. doi: 10.1109/IGARSS46834.2022.9884522.

[23] B. Somers et al., "Automated Extraction of Image-Based Endmember Bundles for Improved Spectral Unmixing," IEEE J. Sel. Top. Appl. Earth Obs. Remote Sens., vol. 5, no. 2, pp. 396–408, Apr. 2012, doi: 10.1109/JSTARS.2011.2181340.

[24] R. Loizzo et al., "PRISMA: The Italian Hyperspectral Mission," in IGARSS 2018 - 2018 IEEE International Geoscience and Remote Sensing Symposium, Valencia, Spain, Jul. 2018, pp. 175–178. doi: 10.1109/IGARSS.2018.8518512.

[25] E. Carmona et al., "Calibration and Validation of the Hyperspectral Mission EnMAP: Results of The Commissioning Phase," in IGARSS 2023 - 2023 IEEE International Geoscience and Remote Sensing Symposium, Pasadena, CA, USA, Jul. 2023, pp. 1030–1033. doi: 10.1109/IGARSS52108.2023.10282471.

[26] R.N. Clark et al., "USGS digital spectral library splib06a, U. S. Geological Survey," Digital Data Series, 231, 2007. http://speclab.cr.usgs.gov/spectral.lib06/